



The suitability of Polish lignite for gasification

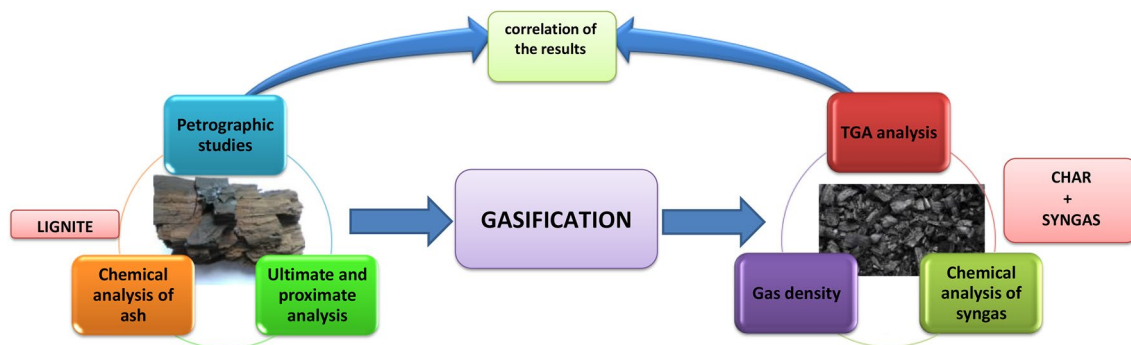
Barbara Bielowicz¹

Received: 15 September 2018 / Accepted: 9 April 2019 / Published online: 16 April 2019
© The Author(s) 2019

Abstract

The article discusses the impact of the lithotype of lignite on the suitability for gasification in CO₂ atmosphere. The research was aimed at determining the influence of lithotype, petrographic composition, and physical and chemical properties of coal on the composition and release of syngas. The examined coals were humic coals. The first step was to determine the impact of lithotype on the degree of carbon conversion at a temperature of up to 815 °C. The gasification process was conducted in the temperature range of 600–1100 °C. During the experiment, two gas samples, used for determining the chemical content of gas, were collected at 950 and 1050 °C, respectively. What is more, continuous monitoring of the gas density during the gasification was carried out. Depending on the lithotype, the content of ash, moisture, and the degree of coalification, the intensity of gas release is different for different temperatures. In addition, it has been found that coals with a high content of poorly gelified xylite and a low ash content are the fastest reacting and the most responsive. The importance of this research lies in determining that the gasification of coal with a low degree of coalification requires technologies carried out at reactor temperatures above 1000 °C.

Graphical abstract



Keywords Lignite · Gasification · Maceral · Petrofactor · Correlation

Introduction

Despite moving away from coal energy, lignite remains among the primary energy sources. However, new, clean, and efficient methods of obtaining energy from lignite are

being sought after. One of them is the gasification process. New installations are being developed and various gasifying agents are used. The most promising gasifying agent is CO₂ (Chmielniak et al. 2015). The issue of CO₂ emissions is the reason why the efficient use of CO₂ is of high importance.

The presented work focuses on determining the suitability of lignite for clean coal technologies, especially for fluidized bed gasification. Exploring the possibility of using Polish coal in these technologies is essential in shaping the energy policy of Poland. In accordance with the energy policy of the EU, numerous studies on the possibilities of using lignite

✉ Barbara Bielowicz
bbiel@agh.edu.pl

¹ AGH University of Science and Technology, Faculty of Geology, Geophysics and Environment Protection, Al. Mickiewicza 30, 30-059 Kraków, Poland

in the power industry, with an emphasis on modern technologies aimed primarily at reducing CO₂ emissions from gasification, are carried out. Currently, in Poland, lignite is generally burned conventionally, which contributes to the increasing environmental pollution. The use of modern gasification technologies would significantly reduce CO₂ emissions during energy production. According to the Energy Policy of Poland until 2040 (Ministry of Energy 2018), coal is still the main element of Poland's energy security and is the basis for the energy balance of the state. However, new methods of coal combustion, i.e., gasification, oxy-combustion, and other clean coal technologies, will be sought after and will be used in order to make the best use of the raw material and to limit the impact on the environment. Lignite deposits are still largely unexploited. The lignite mining itself is generally carried out using the opencast method, which is cheaper than underground mining. This method, given the proper reclamation of post-industrial areas, is not a major threat to the environment. The effective use of lignite in the gasification process requires a number of analyses (Higman et al. 2008). Basic technological analyses are increasingly being accompanied by petrographic analysis. They allow predicting the technological properties and the applications of lignite in a relatively short time (Bielowicz 2012). One of the main objectives is to assess the impact of petrographic composition on the reactivity of lignite. The reactivity of the raw material subjected to the gasification process is one of the basic parameters determining the possibility of the use of lignite in the gasification process. Therefore, a comprehensive study on the influence of the petrographic composition on the reactivity of coal has been carried out. Given the abundant world resources of lignite, there is an urgent need for such studies. This paper aims to fill this gap. Until recently, the reactivity has been studied mainly in bituminous coal (Porada et al. 2017a). However, it should be noted that bituminous coal significantly differs from lignite. Differences between the reactivity of bituminous coal and lignite were discussed by Porada et al. (2017b), who have found that lignite is the most reactive to water vapor. The impact of the petrographic composition of lignite on the underground gasification process was investigated by Akanksha et al. (2017), who have found that lignite, which contains mainly macerals from the huminite and lipinitic groups, is perfectly suited for this process. The role of the petrographic composition in the integrated gasification combined cycle (IGCC) was discussed by Ozer et al. (2017), who studied its effect on the reactivity. Teng et al. (2016) investigated the reactivity of inertinite and xyloid coal in the combustion process. They suggested that the activation energy of xyloid coal is less than that of fusinitic coal.

The research was based on Polish deposits. Ortho-lignite is the most commonly mined coal in Poland. In Poland, there are 95 documented ortho-lignite deposits (PGI-NRI

2017), mainly in the Paleogene and Neogene sediments in the Polish Lowland. In the case of Paleogene and Neogene formations in Poland, 10 groups of coal deposits, of which only three (1st—Mid-Polish lignite seam, 2nd—Lusatian lignite seam, and 3rd—Ścinawa lignite seam), and locally five (including the 2nd group of A-Lubin and 4th group of Dąbrowa), are of economic importance, have been determined. According to the palynological findings of Piwocki and Ziemińska-Tworzydło (1997), the 1st group of Mid-Polish and 2nd group of A-Lubin lignite seams are of Middle Miocene age, while the 2nd—Lusatian, 3rd—Ścinawa, and 4th—Dąbrowa lignite seams are of Lower Miocene age. The geological balance resources (anticipate economic resources) of lignite amount to 23,510.59 Mt, most of which are power coals—23,509.95 Mt, while the remaining 0.64 Mt are sapropelic coals. Other types of lignite, including briquette coal and coal for carbonization, have also been documented (PGI-NRI 2017). However, as of today, they are classified and used as steam coal. Approximately 16% (3690 Mt) of the anticipated economic resources (balance resources) of lignite can be found in the Poznań graben. These include Czempin, Krzywina, and Gostyń deposits. However, the environmental protection of the surface and the high valuation class of agricultural land are the reasons why their potential exploitation is the subject of disputes and conflicts between local communities, environmental organizations, and proponents of exploitation (Kasiński et al. 2006). This can seriously complicate the development of the mentioned deposits.

The anticipated economic resources (balance resources) in the currently exploited deposits amount to 1482.69 Mt or 6.3% of the anticipated economic resources (PGI-NRI 2017). Lignite from these deposits is extracted in five mines (Bełchatów, Turów, Adamów, Konin, and Sieniawa lignite mines). At the current level of consumption, the reserves should last for another several decades.

Poland has large coal reserves—at the current level of production, they should last for many years, and thus coal will continue to be one of the primary energy sources in the future. However, the energy policy of Poland requires the development of clean coal technologies. Therefore, the gasification process provides the opportunity for lignite in Poland. In addition, lignite is of great economic significance in Germany, Greece, Turkey, Serbia, China, and India.

The paper presents the usefulness of this raw material for gasification based on the lithology and petrographic composition. This concept enables rational management of deposits and selecting those where the conversion rate of the gasification process is high. Previous studies were focused on individual deposits, while the presented work is a comprehensive approach to the problem. Therefore, it allows determining differences between individual deposits and, based on the analysis of individual lithotypes, areas with

different suitability for the gasification process within a single deposit. The presented petrographic method for assessing the suitability for gasification can be applied to deposits of various origins.

Experimental

Samples, petrography, proximate and ultimate analyses

The study used 13 lignite samples from Polish deposits, namely the Józwin deposit—three samples, the Turów deposit—two samples, the Sieniawa deposit—three samples, the Bełchatów deposit—three samples, and the Szczerców deposit—two samples (Fig. 1). The samples of various lithotypes of humic lignite were collected. These deposits occur in the 1st, 2nd, and 3rd group of seams.

Additionally, the subbituminous coal sample from the Poreba deposit and 15 samples of medium- and high-rank coals of different petrographic structure (Table 1) were also collected.

The lithotypes of lignite, i.e., sedimentologically homogeneous accumulations of coal, are separated from each other by more or less distinct boundaries, roof and floor, characterized by different physical features. These features reflect the type of starting material and the degree of transformation in the course of peat genesis and diagenesis

(Stach et al. 1982). Determining the lithotype boundaries was based on the macroscopically observed differences in the petrographic composition, a different set of structures and textures of coal, and on surface discontinuities of the sediment. When it comes to lignite, lithotypes with a thickness of up to 10 cm were determined (Kwiecińska and Wagner 1997; Taylor and Glick 1998). The mentioned samples were ground to a grain size lower of < 1 mm and used as a material for polished sections, which were made according to the ISO standards (ISO 7404-2:2009). The maceral analysis was carried out in both reflected white and blue light with the use of a Zeiss microscope and in accordance with the PN-ISO 7404-3:2001 standard. The maceral composition of both lignite and bituminous coal was determined according to the ICCP guidelines (Sýkorová et al. 2005). The macerals from the liptinite group were examined under fluorescent light. The maceral nomenclature for the liptinite group was developed according to (Pickel et al. 2017). The average reflectance of ulminite B and collotelinite was determined under standard conditions, i.e., monochromatic light with a wavelength of 546 nm and immersion oil ($n = 1.518$), using a Zeiss MPM-400 photometer equipped with a MSP-20 system processor. Random reflectance measurements in ortho-lignite were performed on the surface of ulminite B (Sýkorová et al. 2005). The maceral group content analyses were carried out on 500 equally spaced points on the surface of the polished sections.

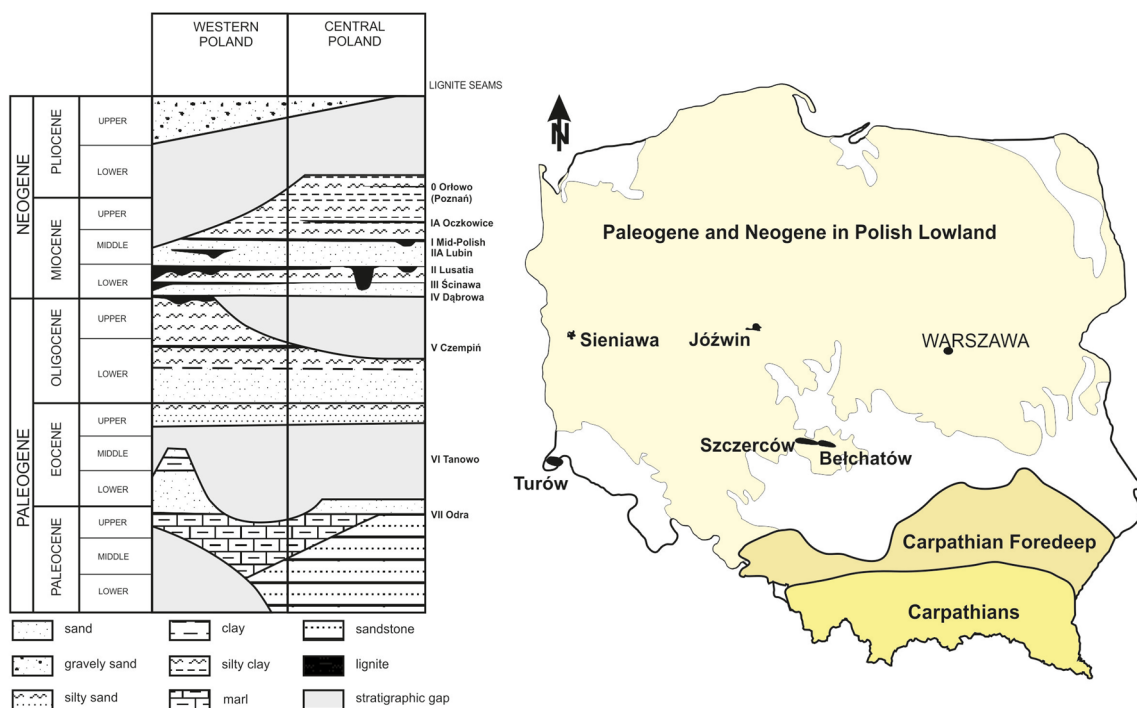


Fig. 1 Location of lignite deposits compared to the tertiary geological map of Poland. Own work based on (Czarnecki et al. 1992; Kasiński et al. 2010; Bielowicz 2012)

Table 1 Summary of samples

Sample no.	Deposit	Seam	Lithotype	Reflectance (%)
1L	Józwin	1st group of Mid-Polish lignite seams	Detritic	0.24
2L	Józwin	1st group of Mid-Polish lignite seams	Xylitic	0.24
3L	Józwin	1st group of Mid-Polish lignite seams	Detro-xylitic	0.24
4L	Turów	3rd group of Ścinawa lignite seams	Xylitic	0.28
5L	Turów	3rd group of Ścinawa lignite seams	Xylo-detritic	0.28
6L	Sieniawa	2nd group of Lusatian lignite seams	Xylo-detritic	0.25
7L	Sieniawa	2nd group of Lusatian lignite seams	Xylitic	0.25
8L	Sieniawa	2nd group of Lusatian lignite seams	Detritic	0.25
9L	Bełchatów	3rd group of Ścinawa lignite seams	Xylo-detritic	0.28
10L	Bełchatów	3rd group of Ścinawa lignite seams	Xylitic	0.28
11L	Bełchatów	3rd group of Ścinawa lignite seams	Detritic	0.28
12L	Szczerców	2nd group of Lusatian lignite seams	Xylitic	0.26
13L	Szczerców	2nd group of Lusatian lignite seams	Xylo-detritic	0.26
17SB	Poręba	Blanowice seam	Detritic	0.35
1B	Jas-Mos	510	Coking coal	1.1
2B	Vietnam	Anthracite	Bright coal	2.3
3B	Janina	119/2	Bright coal	0.5
4B	Janina	119/2	Dull coal	0.5
5B	Janina	203/2	Bright coal	0.5
6B	Janina	203/2	Dull coal	0.5
7B	Bielszowice	510	Bright coal	0.7
8B	Bielszowice	510	Dull coal	0.7
9B	Bogdanka	391	Bright coal	0.6
10B	Bogdanka	391	Dull coal	0.6
11B	Bogdanka	381	Bright coal	0.6
12B	Bogdanka	381	Dull coal	0.6
15B	Bogdanka	385/2	Bright coal	0.6
16B	Bogdanka	385/2	Dull coal	0.6
17B	Wesoła	308	Bright coal	0.6
18B	Wesoła	308	Dull coal	0.6
19B	Bielszowice	405/2	Bright coal	0.7
20B	Bielszowice	405/2	Dull coal	0.7

The gelification index was determined based on the equation (Diessel 1986) and was modified for lignite according to the guidelines by Kalaitzidis et al. (2004) by using formula (1):

$$GI = \frac{(\text{Hulminite} + \text{humocollinite} + \text{densinite})}{(\text{Textinite} + \text{atrinite} + \text{inertinite})} \quad (1)$$

In addition, the petrofactor, which allowed establishing a more general relationship between coal properties and the reactivity, was also calculated. Petrofactor was calculated using formula (2) (Furimsky et al. 1990):

$$Pf = \frac{R_o}{\text{Vitrinite (huminite)} + \text{liptinite} + \frac{1}{3}\text{semifusinite}} \times 1000, \quad (2)$$

where Pf is the petrofactor and R_o is the ulminite B/colotelinite random reflectance.

Proximate and ultimate analyses were carried out for both coal and ash. The samples were ground to a size of 0.2 mm. Proximate analysis covered moisture content, ash content, volatile matter content, and the gross calorific value determination. Ultimate analysis included carbon, hydrogen, nitrogen, and sulfur content determination using a Leco analyzer. The chemical composition of coal and ash was analyzed by ICP-OES/MS at the Bureau Veritas Minerals Laboratory. ICP-MS analysis was performed on a 15-g sample after modified aqua regia digestion (1:1:1 HNO₃/HCl/H₂O) for low to ultra-low determination of both coal and ash.

The alkali index (Sakawa et al. 1982) was calculated using formula (3):

$$AI = A^{ad} \frac{\text{Fe}_2\text{O}_3 + \text{CaO} + \text{MgO} + \text{Na}_2\text{O} + \text{K}_2\text{O}}{\text{SiO}_2 + \text{Al}_2\text{O}_3}. \quad (3)$$

A^{ad} is the ash content in the sample; Fe_2O_3 , CaO , MgO , Na_2O , K_2O , SiO_2 , and Al_2O_3 are the content of particular oxides in the ash, %.

The analysis of the porous texture of the coal samples was carried out at the AGH University of Science and Technology (Faculty of Energy and Fuels) using a Pascal 140 CE porosimeter. The porosimeter works in the pressure range from 0.3 kPa up to 150.0 kPa, which enables the measurement of the pore radii from about 5 nm to 1.8 μm , i.e., macropores and micropores. The apparatus registers the volume of mercury penetrating the pores of the examined material, allowing presenting the dependence curve of open pore volume and pore volume distribution on the pressure applied and radii, respectively. Pore radii corresponding to the specified pressure values are calculated based on the Washburn equation. Taking into account the large spread of the parameters, the results are presented with the use of a logarithmic number system.

All chemical and technological analyses were performed in accordance with ISO standards.

The reactivity studies carried out during coking process have shown that the active site concentration in the molecular structure of chars is dependent on the aromaticity and the degree of molecular ordering in the parent maceral structure (Borrego et al. 1997). The aromaticity factor was obtained from Eq. (4) (van Krevelen 1993):

$$f_a = \frac{1200 \times (100 - V^{daf})}{1240 \times C^{daf}} \quad (4)$$

where f_a is the aromaticity, V^{daf} is the volatile matter on dry ash-free basis, and C^{daf} is the carbon on dry ash-free basis.

The thermogravimetric analysis (TGA) was used to measure the weight loss of the coal sample depending on the temperature and changes over time. The measurement was performed for about 1 g of the sample at a temperature between 32 and 815 °C. The temperature at which the sample gasifies or burns is considered as the limit temperature. The measurement was conducted under CO_2 atmosphere. The TGA analysis was performed for about 150 min, during which the oven was heated from 32 to 815 °C. Exact weight losses were measured at the following temperatures: 200, 400, 600, 700, and 800 °C.

The reactivity of coal to carbon dioxide

The ability of coal to react with carbon dioxide was determined using an apparatus developed by the Central Measurement and Testing Laboratory in Jastrzębie-Zdrój. The studies of this type have already been carried out using fixed

and fluidized bed reactors. The above-mentioned methods were applied in order to control the condition of samples and process parameters. The applied research method assumed a particle size from 0.2 to 3.0 mm. The ground samples were evenly spread on metal trays and dried at 40 °C. After 4 h, they were conditioned in a laboratory atmosphere until reaching constant weight (equilibrium with atmospheric moisture), which was checked every 2 h. The obtained laboratory sample in the air-dry state was used to isolate a subsample for physicochemical determinations and 100 g subsamples for the determination of reactivity. In order to obtain the desired fraction (0.2–3.0 mm), the prepared subsamples were sieved through a 0.2-mm sieve and protected in sealed packages.

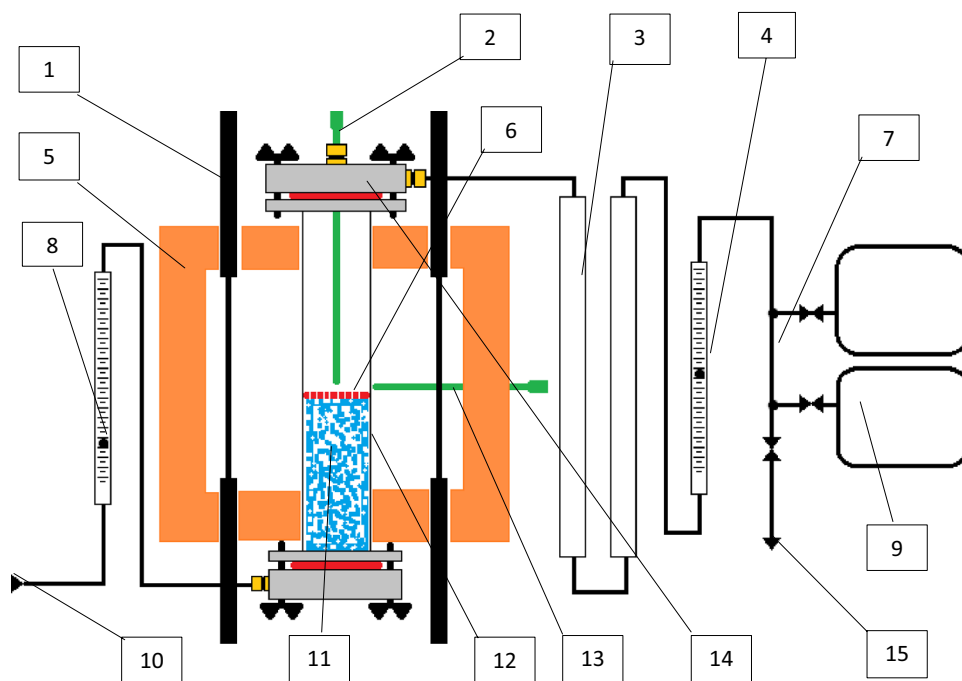
The reactivity was examined in the reactor, whose design is shown in Fig. 2.

The gasification of coal in CO_2 atmosphere in the reactor takes place at a temperature of 600 °C to 1100 °C at atmospheric pressure. To heat the sample to the mentioned temperature, a furnace with silicate heaters has been used. In addition, carbon dioxide was used as an oxidizing gas. The coal reactivity analysis was carried out in an indirectly heated reactor. In order to remove the drying and preliminary degassing products that do not react with CO_2 at low temperatures, the samples were preheated to 600 °C. After the initial degassing, the reactor was heated to 1100 °C for 18–19 min. To avoid the release of significant amounts of tar during degassing, a nominal sample mass of 5.00 g was assumed. During the chromatographic studies, the gas samples were collected using standard 3 dm³ Tedlar bags. There were two gas sample collection points for lignites. The composition of samples collected from both sampling points was analyzed by means of gas chromatography. Due to the fact that the most intensive processes occurred at temperatures of 950–1100 °C, the first sample was collected when the temperature reached 950 °C, while the second at the temperature of 1050 °C.

Statistical analysis

The obtained results of chemical, technological, and petrographic analysis were correlated with each other. The relationship between the starting material, obtained products, and reactivity was examined based on the results of correlation analysis. In order to determine correlations between individual parameters, the analysis of correlation and regression has been used. The Pearson (r) correlation coefficients were determined, which was followed by the evaluation and testing of the statistical significance of this factor. The test of statistical significance has been performed using the Student's t distribution. The analysis used Statistica and Excel software.

Fig. 2 Construction of the reactor for reactivity analysis. 1—Silicate heaters, 2—the main thermocouple (K), 3—absorbers filled with glass wool, 4—post-reaction gas rotameter, 5—thermal insulation, 6—chromium-nickel sieve bottom, 7—valve set, 8—oxidation gas rotameter, 9—Tedlar gas bags, 10—the inlet of the oxidizing gas, 11—porous material, 12—ceramic pipe, 13—thermocouple of the furnace, 14—gas from the reactor, 15—the outlet for excess post-reaction gas



The characteristics of the examined coal

The examined lignite is humic coal (ortho-lignite), while the huminite reflectance ranges from 0.24 to 0.28%. The following lithotypes were examined: detritic coal, xylo-detritic coal, detro-xylitic coal, and xylitic coal.

Xylitic coal is a layered or lenticular accumulation of xylites, which represent at least 90% of its volume. Accompanying components may include humic detritus or dispersed lipid or mineral matter. The xylites include all fragments with wood morphology and with a diameter of at least 1 cm. According to the classification (Kwiecińska and Wagner 1997), three structural varieties of xylites were determined: fibrous, brittle, and loose. Detritic coal is built of fine humic particles (detritus), forming the more or less macroscopically homogeneous mass. It can contain up to 10% by volume of other component (e.g., xylites, fusain, granular accumulations of resinite or gelinite, minerals, etc.). Detro-xylitic and xylo-detritic coal belong to complex (heterogeneous) lithotypes built from xylites and humic detritus. These lithotypes form thicker layers in coal seams, which can be distinguished based on their petrographic composition and texture. The detro-xylitic coal is dominated by xylites. On the other hand, the xylo-detritic coal is dominated by detritus. The admixtures (up to 10% by vol.) include: lipid detritus, lenticular accumulations of this material (mainly resin grains, sapropelic xylites, sapropelic lenses, accumulations of leaves and bark), fusains, detritus of carbonized plants, gel lenses, and accumulations of minerals.

The petrographic composition of different coal samples depends on their lithological development (Table 2). The

petrographic composition of the examined coal is dominated by macerals from the huminite group. The share ranges from 73.6 to 97.1%. The share of the macerals from the inertinite group in the examined samples is up to 4%. The only exception is the sample of xylitic coal from the Józwin deposit, containing 19.9% of macerals from the inertinite group (mainly fusinite). The liptinite group in the tested samples ranges from 1.7 to 8.5%. The detailed petrographic composition of the examined coal is presented in Table 2.

The examined samples are mainly macerals of the huminite group, which are characterized by a higher oxygen content and lower carbon content compared to both inertinite and liptinite (Cronauer et al. 1992). A relatively large number of aliphatic groups have been observed in the examined ortho-lignite samples. The H/C and O/C atomic ratios and the amount of methoxyl groups decrease, while the aromaticity and the content of carboxyl groups increase as a result of biochemical processes (Russell and Barron 1984). At the same time, it should be noted that the highly phenolic signatures of the lignin-derived material within the huminite, with a minor content of aliphatic groups, are characteristic for huminite (Stankiewicz et al. 1996). This chemical composition promotes the gasification process.

The porous coals, consisting largely of xylite, are the fastest reacting ones. This is related to the fact that their chemical bonds break down more easily. Meanwhile, xylite has a higher proportion of aliphatic components. The xylite with a lower degree of coalification is mainly built of textinite. Textinite consists of humic substances and remains of cellulose and lignin. During the gasification process, textinite produces high yields of both tar and gas. This is related to its

Table 2 Petrographic composition of lignite

Sample	1L	2L	3L	4L	5L	6L	7L	8L	9L	10L	11L	12L	13L
Deposit	Józwin	Józwin	Józwin	Turów	Turów	Sieniawa	Sieniawa	Sieniawa	Belchatów	Belchatów	Belchatów	Szczerców	Szczerców
Lithotype	Detritic	Xylitic	Detro-xylitic	Xylitic	Xylo-detritic	Xylo-detritic	Xylitic	Detritic	Xylo-detritic	Xylitic	Detritic	Xylitic	Xylo-detritic
Maceral													
Textinite	2.8	5.3	7.0	18.1	1.3	2.4	6.9	5.2	17.9	75.0	7.8	82.7	4.4
Ulminite	2.8	28.0	27.8	55.2	34.2	30.4	40.6	2.4	13.4	5.3	12.8	8.0	15.9
Attrinite	49.9	21.6	17.5	4.2	16.8	18.9	16.5	29.7	21.3	5.3	32.2	2.0	33.8
Densinite	33.6	18.3	28.6	15.4	41.6	40.2	22.1	46.2	36.2	4.8	39.1	2.0	19.1
Corphuminite	0.5	0.0	0.0	0.0	0.0	0.0	0.0	0.8	0.0	0.0	0.0	0.0	0.4
Gelinite	1.0	1.5	8.6	1.2	0.5	1.8	5.1	0.4	1.1	5.3	0.6	2.4	0.0
Sporinite	0.5	0.3	1.0	0.3	0.7	0.6	0.2	1.0	0.3	0.2	0.5	0.1	0.6
Cutinite	0.2	0.1	0.1	0.1	0.3	0.1	0.0	0.2	0.2	0.1	0.2	0.1	0.2
Resinite	0.7	1.0	0.5	2.1	2.0	1.6	2.1	1.5	0.8	1.1	0.5	1.4	4.6
Suberinite	0.3	0.1	0.1	0.2	0.0	0.1	0.0	0.6	0.2	0.1	0.2	0.0	0.2
Alginite	0.1	0.0	0.1	0.0	0.0	0.0	0.0	0.3	0.1	0.0	0.0	0.0	0.1
Liptodetrinite	0.5	0.2	0.2	0.0	0.4	0.5	0.0	0.4	1.1	0.3	1.2	0.1	2.8
Fusinite	1.3	14.0	2.4	0.0	0.3	0.0	0.0	0.4	0.7	1.0	0.6	0.4	2.8
Semifusinite	0.8	0.0	0.0	0.0	0.0	0.0	0.0	0.0	0.4	0.0	0.0	0.0	0.0
Funginite	0.5	0.0	0.0	0.0	0.0	0.0	0.0	0.4	0.0	0.0	0.0	0.0	0.0
Micrinite	0.0	0.0	0.0	0.0	0.0	0.0	0.0	0.0	0.0	0.0	0.0	0.0	0.0
Inertodetrinite	0.0	4.7	1.3	0.3	0.5	0.6	0.0	0.8	0.7	0.5	0.9	0.4	4.0
Pyrite	1.0	0.0	0.0	0.0	0.0	0.0	0.0	0.8	0.4	0.0	1.6	0.0	0.8
Carbonates	0.0	0.0	0.0	0.0	0.0	0.0	0.0	0.0	0.4	0.0	0.0	0.0	0.0
Quartz+Clays	3.6	3.6	4.6	3.0	1.3	2.7	6.4	8.8	4.8	1.0	1.6	0.4	10.3
Huminite	90.6	74.8	89.6	94.0	94.5	93.7	91.3	84.8	89.9	95.8	92.7	97.1	73.6
Inertinite	2.5	19.9	3.8	0.3	0.8	0.6	0.0	1.6	1.9	1.5	1.6	0.8	6.8
Liptinite	2.3	1.7	2.0	2.7	3.4	2.9	2.3	4.0	2.7	1.8	2.6	1.7	8.5
Mineral matter	4.6	3.6	4.6	3.0	1.3	2.7	6.4	9.6	5.6	1.0	3.1	0.4	11.1
Telohuminite	5.6	33.3	34.8	73.2	35.5	32.9	47.5	7.6	31.3	80.3	20.7	90.7	20.3
Detrohuminite	83.5	40.0	46.2	19.6	58.4	59.0	38.7	75.9	57.4	10.2	71.4	4.0	52.9
Gelohuminite	1.0	1.5	8.6	1.2	0.5	1.8	5.1	0.4	1.1	5.3	0.6	2.4	0.0
GI	0.7	1.0	2.3	3.2	4.0	3.3	2.9	1.3	1.2	0.2	1.3	0.1	0.8
TPI	0.1	1.0	0.7	3.5	0.6	0.5	1.1	0.1	0.5	5.1	0.3	13.4	0.4
Petrofactor	2.58	3.13	2.62	2.89	2.86	2.59	2.67	2.82	3.02	2.87	2.94	2.63	3.17

high content of cellulose derivatives and/or resin. The textinite char yield is rank dependent (Süss et al. 1968). In the case of more gelified xylitic coal with a higher degree of carbonization, the dominant component is ulminite. Ulminite produces lower yields of tar and gas and higher amounts of char when compared to textinite. Compared with textinite, ulminite reacts at lower temperatures (Kurtz 1981). Based on the obtained results, it can be stated that both textinite and ulminite speed up and favor the gasification of coal.

The coal with a high detrohuminite (especially attrinite) content is the least responsive. At early stages of coalification, detrohuminite is derived from demethylated dehydrated lignin monomers mixed with lipids, such as polymethylene long-chain acids, esters, or triterpenoids of higher plant and microbial origin (Taylor et al. 1982). Attrinite, a maceral from the huminite group (detrohuminite subgroup), consists of a mixture of fine huminitic particles (< 10 µm) with variable shape and spongy to porous ungelified amorphous huminitic substances. Attrinite consists of humic substances and cellulose and lignin residues. A lower reactivity of

detrohuminite macerals, and a low content of bitumens, was observed by Süss et al. (1968) and Shibaoka (1982).

The moisture content on air-dry basis in the examined samples varies from 4.6% in xylo-detritic coal from Szczerców deposit to 12.0% in detritic coal from Bełchatów deposit (Table 3). The ash content (dry basis) in the examined coal ranges from 2.3 to 46.2%. It can be observed that in some seams the ash content is clearly higher in the case of detritic coal. The volatile matter decreases with the rank of coal from 49.4 to 63.1%. The sulfur content (dry basis) in the examined samples is not clearly related to the lithotype or rank of coal and is in the range from 0.5 to 3.9%. The carbon content in dry, ash-free basis varies with the degree of coalification from 61.8 to 70.7%. The porosity ranges from 8.4 to 35.9% and is largely dependent on the lithotype and the amount of mineral matter in coal. The oxide composition of the ash depends on the deposit. The Józwin and Turów deposits are dominated by SiO₂ and Al₂O₃, while the Sieniawa and Szczerców by CaO.

Table 3 Proximate and ultimate analyses of the examined lignite

	1L	2L	3L	4L	5L	6L	7L	8L	9L	10L	11L	12L	13L
Moisture M_t^{ad} (%)	7.6	8.2	9.6	8.4	10.0	10.5	7.6	9.3	9.8	8.7	12.0	11.6	4.6
Ash A^{db} (%)	46.2	6.2	24.6	5.0	3.8	6.9	2.3	6.5	16.2	7.2	19.8	2.7	23.2
Volatile matter V^{daf} (%) ^f	56.2	58.8	56.9	57.4	56.8	55.8	63.1	58.0	55.8	56.2	55.4	64.2	49.4
Sulfur S_t^{db} (%)	1.6	1.6	2.8	1.9	0.8	1.0	0.5	0.5	1.7	3.6	3.6	1.0	3.9
Gross calorific value GCV (MJ/kg)	23.9	25.9	26.1	28.9	29.2	26.2	24.8	26.3	25.6	26.9	25.5	26.7	27.6
Net calorific value NCV (MJ/kg)	9.8	18.1	14.8	21.8	20.9	18.8	20.2	12.7	18.0	19.0	14.4	17.54	18.7
Carbon C^{daf} (%)	64.0	64.9	66.3	69.2	70.7	66.0	61.8	66.5	65.7	63.4	65.4	65.0	67.4
Hydrogen H^{daf} (%)	4.7	5.3	5.1	5.8	6.0	5.2	5.6	5.3	5.0	5.2	4.8	5.8	5.2
Nitrogen N^{daf} (%)	0.6	0.2	0.4	0.4	0.5	0.5	0.1	0.8	0.7	0.2	0.9	0.1	0.9
Oxygen O^{daf} (%)	27.7	27.8	24.5	22.5	22.0	27.2	31.9	26.9	26.6	27.3	24.4	28.1	21.5
Total cumulative volume (mm ³ /g)	258.5	196.0	290.2	95.5	259.9	400.1	303.0	198.5	57.4	170.5	127.5	283.3	216.7
Total porosity (%)	33.4	25.0	31.5	11.5	26.5	35.9	31.6	22.9	8.4	19.9	18.3	28.6	25.9
Bulk density (g/cm ³)	1.3	1.3	1.1	1.2	1.0	0.9	1.0	1.2	1.5	1.2	1.4	1.0	1.2
Apparent density (g/cm ³)	1.9	1.7	1.6	1.4	1.4	1.4	1.5	1.5	1.6	1.5	1.8	1.4	1.6
Aromaticity factor fa	0.7	0.6	0.6	0.6	0.6	0.6	0.6	0.6	0.7	0.7	0.7	0.5	0.7
Ash composition													
SiO ₂	66.8	37.4	64.3	19.3	18.2	20.4	–	7.4	25.5	19.7	20.4	18.4	63.4
Al ₂ O ₃	16.9	9.9	3.0	15.0	19.0	3.5	–	3.2	16.7	13.8	13.9	7.4	11.8
Fe ₂ O ₃	2.2	7.8	6.3	21.9	6.2	11.7	–	17.6	7.2	8.6	9.7	7.6	16.4
MgO	1.6	3.5	2.3	6.4	11.0	2.4	–	2.1	2.2	1.6	1.3	2.2	0.3
CaO	6.1	18.1	9.4	4.9	8.4	26.1	–	30.0	23.6	24.4	24.5	25.6	1.2
Na ₂ O	0.1	0.3	0.1	7.8	12.3	0.3	–	0.1	0.5	0.1	0.0	0.2	0.1
K ₂ O	0.6	0.6	0.2	1.2	1.0	0.3	–	0.1	0.2	0.4	0.2	0.4	0.8
TiO ₂	1.7	0.6	0.5	1.6	2.4	0.3	–	0.3	0.6	0.8	0.7	0.5	2.9
P ₂ O ₅	0.0	0.3	0.0	0.2	0.2	0.0	–	0.0	0.2	0.2	0.1	0.1	0.1
MnO	0.1	0.1	0.2	0.0	0.0	0.1	–	0.2	0.2	0.1	0.1	0.1	0.0
Cr ₂ O ₃	0.2	0.1	0.2	0.1	0.1	0.0	–	0.0	0.0	0.1	0.0	0.1	0.0
Others	3.8	21.2	13.6	21.5	21.2	34.9	–	38.9	23.1	30.3	29.1	37.6	2.9
Alkali index	5.4	3.6	6.1	5.7	3.6	10.5	–	27.7	11.6	6.9	18.0	3.3	5.5

Determining the reactivity of coal

The main purpose of the study was to determine the quantity and composition of gases released from coal during heating. The main phenomenon observed during the experiment is pyrolysis, while the gasification process starts at 900 °C (Solomon and Hamblen 1985; Tremel and Spliethoff 2013). The first study was presented by Solomon and Hamblen (1985), who claimed that the boundary between the pyrolysis process and lignite gasification is around 900 °C. These studies have been confirmed by Tremel and Spliethoff (2013). The pyrolysis process is associated with the destructive distillation of organic substances by thermal energy in the absence of air. The tested coal was gasified in CO₂ atmosphere.

Ladner (1988) has determined several stages of coal heating:

1. Below 350 °C, where the volatiles are mainly a result of evaporation rather than thermal degradation; in addition, water, volatile organics, hydrocarbons, and aromatic hydrocarbons such as benzene, toluene, and even HCl are also released.
2. 400–750 °C, the main area of thermal decomposition, commonly referred to as the low-temperature carbonization area; the products are mainly gas and char (tar, liquor, and hydrogen are produced in lower amounts).

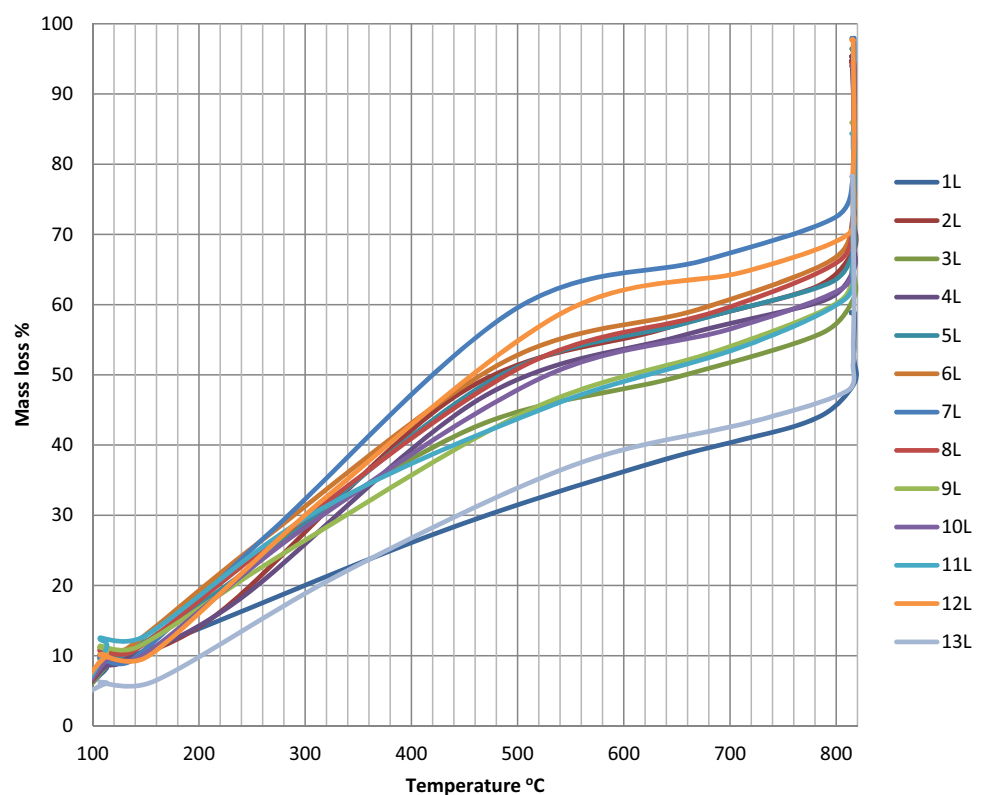
3. 750–900 °C, medium temperature carbonization; gas, char, tar, liquor, and hydrogen are released.
4. 900–1100 °C, the so-called high-temperature carbonization region, where appreciable thermal cracking of volatiles is taking place.
5. Above 1650 °C, where acetylene formation is favored.

It is clearly visible that the temperature is the most important parameter affecting the pyrolysis process. As a consequence, it has a direct impact on the produced char, liquids, and gases.

The first stage of the study examined the weight loss of carbon during the heating to a temperature of 815 °C in CO₂ atmosphere.

Figure 3 presents how the individual samples responded to increasing temperature. A clear relationship between the lithotype of coal and the speed of reaction can be observed. Detritic coal (sample 1L—detritic Józwin, 13L—xylo-detritic Szczerców) with high mineral matter content loses weight more slowly. However, xylitic coal (7L—xylitic Sieniawa, 12L—xylitic Szczerców), with high porosity starts to react at lower temperatures; at temperatures of 500–600 °C, 60% of the sample mass is converted. Interestingly, xylitic coal of higher rank ($R_o=0.28\%$), e.g., from the Turów and Bełchatów deposits, does not react as easily as the lower-rank xylitic coal. Generally, it can be concluded that a 50% reaction at a temperature of 600 °C was observed in the majority of the tested samples.

Fig. 3 Weight loss of lignite heated in a CO₂ atmosphere



Comparing the weight losses for lignite with and coals of higher rank (Fig. 4), it is clearly visible that ortho-lignite is losing mass at lower temperatures. In addition, the final weight loss is higher for lignite. This is related to the lower amount of chemical bonds in lignite, which are difficult to break down.

In the next stage of the study, the amount and composition of gas released at 600–1100 °C in a CO₂ atmosphere was determined and subjected to an analysis. Figure 5 presents the relationship between the gas flow and increasing temperature. In some of the samples (4L, 5L, and 13L), two phases of increased gas release, at temperature ranges of 700–800 °C and 900–1100 °C, are clearly visible. This applies to xylitic and xylo-detritic coal samples. At the same time, the mentioned samples are characterized by the highest carbon content and gross calorific value. It is suggested that aliphatic hydrocarbons, which due to the higher degree of carbonization are more strongly bound to the carbon skeleton and are not released during the initial degassing process, are released in the first phase. Gas released at temperatures between 900 and 1100 °C is the result of thermal cracking of lignite and the formation of syngas. The highest gas flow in this phase is observed mainly for xylitic coal (samples 2L, 10L, and 7L) and xylo-detritic coal (samples 6L and 5L).

In the case of coal with random vitrinite reflectance higher than 0.5%, two phases of gas release were clearly observed in the flow analysis. The first phase has a maximum

temperature of approximately 900 °C, and the second phase has the temperature range from 950 to 1100 °C (Fig. 6). The first phase involves the degassing of coal, when volatile components, consisting of gas products and tar vapor formed during the thermal decomposition of solid fuel without air access, are released. The amount of volatiles decreases with increasing coalification of solid fuels, which can be observed at temperatures of 950 °C and higher (Fig. 6). This is associated with changes in the organic structure of the carbonaceous matter during the coalification process, the reduction of heteroatoms, and the increasing share of heat-resistant, aromatic core of structural units at the expense of the peripheral part. During the second phase, mostly CO and CO₂, accompanied by limited amounts of methane, are released. The first phase, at temperatures of up to 950 °C, is related to devolatilization, while the second phase of gas release is associated with the gasification process (Solomon et al. 1993). The gasification starts after the completion of the devolatilization process. In the second phase, when the gasification process takes place, the most commonly observed are heterogeneous reactions with coal, Boudouard, and hydrogenation reactions (Higman et al. 2008). Meanwhile, the largest gas density for low-rank coal is observed at temperatures in the range 800–1000 °C, which indicates that the lignite gasification process occurs at lower temperatures than for medium- and high-rank coal.

Fig. 4 Weight loss in coal samples with different degree of coalification

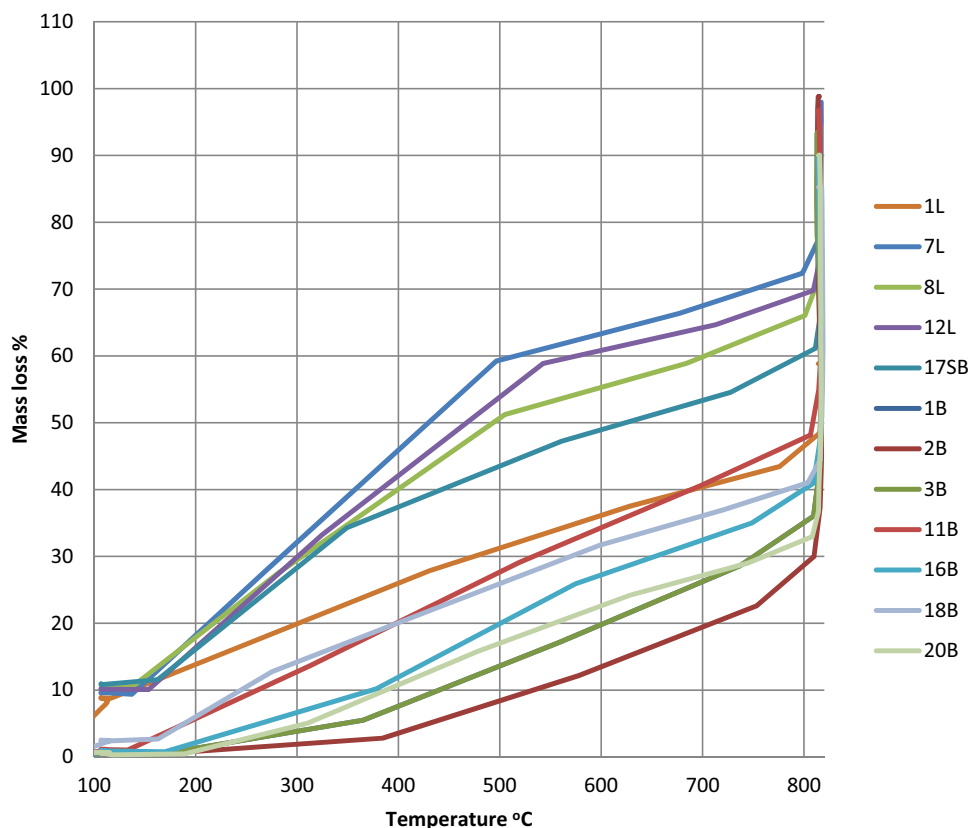


Fig. 5 Gas flow (dm^3/h) as a function of temperature in the Polish lignite

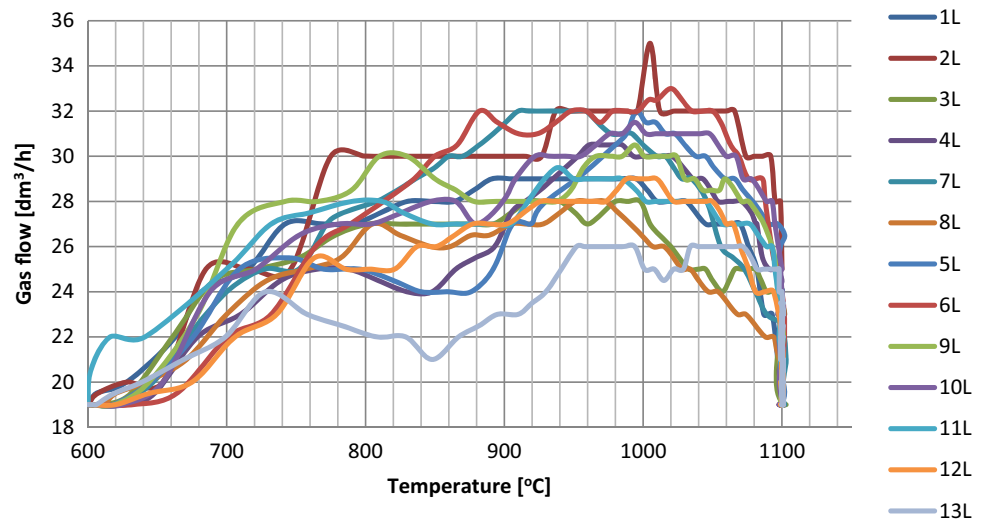
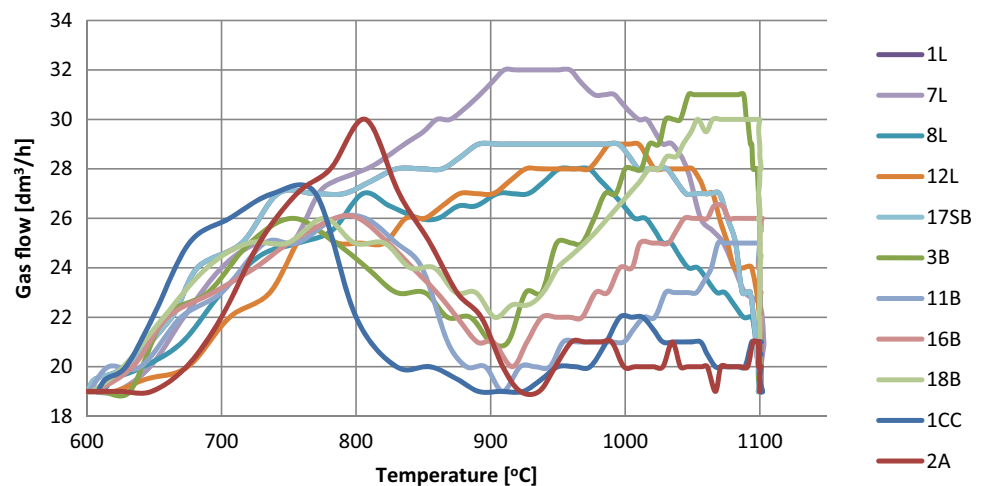


Fig. 6 Gas flow (dm^3/h) as a function of temperature with a different rank of coal



The percentage of H_2 , O_2 , CO , CO_2 , CH_4 , N_2 , and H_2S was determined in the gas samples collected at the temperatures of up to $950\text{ }^\circ\text{C}$ and $1050\text{ }^\circ\text{C}$ (Fig. 7).

At a temperature up to $950\text{ }^\circ\text{C}$ ($600\text{--}900\text{ }^\circ\text{C}$), the hydrogen generation in the examined lignite is maximally up to 3%, as observed in the case of detritic coal sample from the Sieniawa deposit. In addition, xylic coal from the Szczerców and Sieniawa deposits contained 2.8% of hydrogen (Fig. 7). In the remaining samples, the H_2 content slightly exceeds 2%. At a temperature of $950\text{--}1050\text{ }^\circ\text{C}$, the amount of generated H_2 is much lower compared to amounts generated under lower temperature conditions (up to $900\text{ }^\circ\text{C}$). The lowest amount of H_2 (0.2%) was released in the case of detritic coal with mineral matter from the Józwin deposit. In contrast, the highest amount of H_2 (1.6%) released at a temperature of up to $1050\text{ }^\circ\text{C}$ was reported for xylo-detritic coal from the Sieniawa deposit. In the remaining samples, these contents vary from 0.5 to 1.4%.

When it comes to gases resulting from the gasification processes carried out at temperatures between 600 and $950\text{ }^\circ\text{C}$ and up to $1050\text{ }^\circ\text{C}$, the CH_4 and hydrogen contents are higher for the former than for the latter. The highest contents (up to 0.5%) are observed for xylo-detritic coal from the Turów and Sieniawa deposits. At temperatures between 950 and $1050\text{ }^\circ\text{C}$, the methane content in the examined gas does not exceed 0.3%.

Both the reactivity and the amount of released gas are affected by different properties of coal. It is commonly accepted that the reactivity of coal decreases with increasing degree of coalification, while the reactivity of low-rank coals can vary (Hashimoto et al. 1986; Miura et al. 1987).

To determine the relationship between the yield of individual gases at temperatures between 950 and $1050\text{ }^\circ\text{C}$ and proximate, ultimate, and petrographic parameters, a correlation analysis has been performed. Table 4 presents the

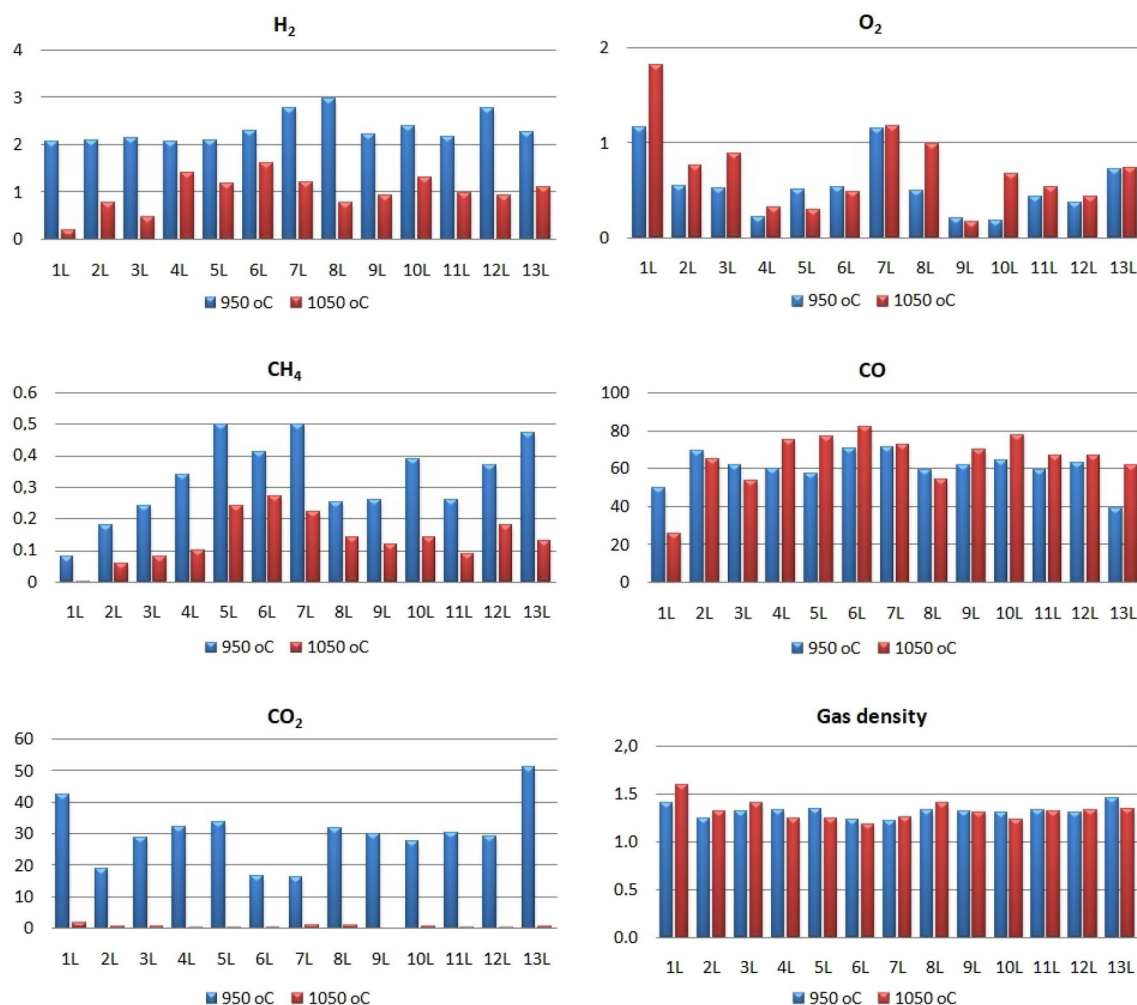


Fig. 7 Percentage of H₂, O₂, CO, CO₂, CH₄ (vol%), and gas density (kg/m³), in the gas samples collected at the temperatures of up to 950 °C and 1050 °C

results of the correlation and the Pearson correlation coefficients. It presents only significant relationships ($p=0.05$).

The results of the analysis have confirmed that the gas composition is affected by different parameters depending on different temperature conditions (temperatures until 950 and 1050 °C).

Higher moisture content at temperatures up to 200 °C has a significant impact on the weight loss of coal. High ash content negatively affects weight loss up until the temperature of 815 °C. At the same time, the CH₄ content decreases with increasing ash content up until the temperature of 950 °C. The ash content has a negative impact on the H₂, CO, and CH₄ contents in the case of gas produced at 950–1050 °C and the CO₂ and H₂S contents in the syngas. The volatile matter content in lignite significantly affects weight loss during heating. In addition, an increase in the volatile matter content in synthetic gas is accompanied by an increase in H₂, CO, and CH₄ contents and a decrease in CO₂ and

H₂S contents. This is related to the fact that volatiles are mainly composed of hydrogen, carbon monoxide, carbon dioxide, water vapor (e.g., crystallization water), methane, and other hydrocarbons (Speight 2016). Higher net calorific value, gross calorific value, carbon, and hydrogen contents significantly affect weight loss during heating and increase the CH₄ content in the gas produced at a temperature of up to 950 °C. In the case of gas produced at 950–1050 °C, higher net calorific value and gross calorific value increase the H₂ and CO content, while reduce the CO₂ content in the gas. The higher the total porosity of lignite, the higher the O₂ content in the syngas. The petrographic composition is of no great significance to the syngas composition. It was reported that the CO content decreases, while the CO₂ and H₂S contents increase with increasing content of macerals from the liptinite group; this is observed up to a temperature of 950 °C. It has been shown that semifusinite negatively affects the conversion process. In addition, an

Table 4 Relationship between proximate and ultimate parameters of coal and gas composition

Gas component	600–950 °C																
	H ₂	O ₂	CO	CO ₂	CH ₄	N ₂	H ₂ S	Gas density	H ₂	O ₂	CO	CO ₂	CH ₄	N ₂	H ₂ S	Gas density	
<i>M^{ad}</i>	0.58	-	-	-	-	-	-0.66	-	-	-	-	-	-	-	-	-	-
<i>A^{db}</i>	-	-	-	-	-0.62	-	-	-	-0.67	-	-0.75	0.76	-0.56	-	0.65	0.76	-
<i>V^{ad}</i>	0.55	-	0.58	-0.58	0.53	-	-0.66	-0.60	-	0.62	-0.63	-	-	-	-0.69	-0.63	-
<i>S_r^{ad}</i>	-	-	-	-	-	-	0.67	-	-	-	-	-	-0.58	-	0.83	-0.01	-
GCV	-	-	-	-	0.70	-	-	-	0.69	0.73	-0.73	-	-	-	-	-0.73	-
NCV	-	-	-	-	0.70	-	-	-	0.69	0.72	-0.73	-	-	-	-	-0.73	-
<i>C^{ad}</i>	-	-	-	-	0.66	-	-	-	0.68	0.73	-0.74	-	-	-	-	-0.74	-
<i>H^{ad}</i>	-	-	-	-	0.69	-	-	-	0.61	0.66	-0.68	-	-	-	-	-0.68	-
<i>O^{ad}</i>	0.66	-	0.63	-0.66	-	-	-	-0.69	-	-	-	-	0.58	-	-0.71	-	-
Total porosity (%)	-	0.72	-	-	-	-	-	-	-	-	-	-	-	-	-	-	-
Petrographic composition																	
W	-	-	-	-	-	-	-	-	-	-	-	-	-	-	-	-	-
I	-	-	-	-	-	-	-	-	-	-	-	-	-	-	-	-	-
L	-	-	-0.75	0.67	-	-	0.83	0.66	-	-	-	-	-	-	-	-	-
<i>R_o</i>	-	-0.60	-	-	-	-	-	-	-	-0.66	-	-	-	-	-	-	-
Semifusinite	-	-	-	-	-0.61	-	-	-	-0.60	-0.71	0.71	-	-	-	-	0.71	-
<i>f_a</i>	-	-	-0.54	-	-	-	0.65	-	-	-	-	-	-	0.62	-	-	-
Ash composition																	
SiO ₂	-	0.66	-	-	-	-	-	-	-0.59	0.58	-0.65	0.64	-	-	-	0.64	-
Al ₂ O ₃	-	-	-	-	-	-	-	-	-	-	-	-	-	-	-	-	-
Fe ₂ O ₃	-	-	-	-	-	-	-	-	-	-	-	-	-	-	-	-	-
MgO	-	-	-	-	-	-	-	-	-	-	-	-	-	-	-	-	-
CaO	0.61	-	0.64	-0.63	-	-	-	-0.66	-	-	-	-	-	-	-	-	-
Na ₂ O	-	-	-	-	-	-	-	-	-	-	-	-	-	-	-	-	-
K ₂ O	-	-	-	-	-	-	-	-	-	-	-	-	-	-	-	-	-
TiO ₂	-	-	-0.77	0.76	-	-	0.61	0.77	-	-	-	-	-	-	-	-	-
P ₂ O ₅	-	-	-	-	-	-	-	-	-	-	-	-	-	-	-	-	-
MnO	-	-	-	-	-	-	-	-	-	-	-	-	-	-	-	-	-
Cr ₂ O ₃	-	0.60	-	-	-	-	-	-	-0.67	0.69	-0.65	0.63	-	-	-0.58	0.32	-
Ba	-	-	-	-	-	-	-	-	-	-	-	-	-	-	-	-	-
Ni	-	0.56	-	-	-	-	-	-	-	-	-	-	-	-	-	-	-
Sc	-	-	-	-	0.57	-	-	-	-	-	-	-	-	-	-	-	-
Alkali index	-	-	-	-	-	-	-	-	-	-	-	-	-	-	-	-	-
Gas composition up to 950 °C (%)	-	-	-	-	-	-	-	-	-	-	-	-	-	-	-	-	-

Table 4 (continued)

Gas component	600–950 °C															
	H ₂	O ₂	CO	CO ₂	CH ₄	N ₂	H ₂ S	Gas density	H ₂	O ₂	CO	CO ₂	CH ₄	N ₂	H ₂ S	Gas density
H ₂	-	-	-	-	-	-	-	-	-	-	-	-	-	-	-	-
O ₂	-	-	-	-	-	-	-	-	0.84	-	-0.58	-	-	-	-	-
CO	-	-	-	-0.99	-	0.54	-0.67	-0.99	-	-	-	-0.54	-	-	-0.63	-
CO ₂	-	-	-0.99	-	-	-0.65	0.63	1.00	-	-	-0.54	0.56	-	0.61	0.55	-
CH ₄	-	-	-	-	-	-	-	-	0.73	-	0.64	-0.66	0.79	-	-0.67	-
N ₂	-	-	0.54	-0.65	-	-	-	-0.64	-	-	-	-	-	0.67	-	-
H ₂ S	-	-	-0.67	0.63	-	-	-	0.62	-	-	-0.54	0.56	-	-	0.66	-
Gas density at 25 °C	-	-	-0.99	1.00	-	-0.64	0.62	-	-	-	-0.54	0.56	-	0.63	0.56	-
Gas composition up to 1050 °C (%)	-	-	-	-	-	-	-	-	-	-	-	-	-	-	-	-
H ₂	-	-	-	-	0.73	-	-	-	-	-0.61	0.91	-0.93	0.58	-	-	-0.93
O ₂	-	0.84	-	-	-	-	-	-	-0.61	-	-0.80	0.73	-	-	-	0.73
CO	-	-0.58	-	-0.54	0.64	-	-	-0.54	0.91	-0.80	-	-0.99	-	-	-	-0.99
CO ₂	-	-	-0.54	0.56	-0.66	-	-	0.56	-0.93	0.73	-0.99	-	-	-	-	1.00
CH ₄	-	-	-	-	0.79	-	-	-	0.58	-	-	-	-	-	-	-
N ₂	-	-	-	-	-	0.67	-	-	-	-	-	-	-	-	-	-
H ₂ S	-	-	-0.63	0.61	-	-	0.66	0.63	-	-	-	-	-	-	-	-
Gas density at 25 °C	-	-	-	0.55	-0.67	-	-	0.56	-0.93	0.73	-0.99	1.00	-	-	-	-
TGA—mass loss at a given temperature	-	-	-	-	-	-	-	-	-	-	-	-	-	-	-	-
200	-	-	0.66	-0.65	-	-	-0.71	-0.65	-	-	-	-	-	-	-	-
400	-	-	0.80	-0.81	-	-	-0.59	-0.82	-	-	0.61	-0.63	-	-0.74	-0.62	-
600	0.57	-	0.70	-0.70	-	-	-	-0.73	-	-	0.62	-0.63	-	-0.75	-0.63	-
700	0.55	-	0.74	-0.74	-	-	-0.55	-0.76	-	-	0.63	-0.64	-	-0.76	-0.64	-
800	0.56	-	0.78	-0.78	-	-	-0.58	-0.80	-	-	0.63	-0.64	-	-0.77	-0.63	-
815	-	-	-	-	0.60	-	-	-0.55	0.68	-	0.77	-0.78	-	-0.62	-0.78	-

increase in the semifusinite content reduces weight loss of the examined sample and the CH₄ and H₂ contents in the syngas. Compared to other maceral groups, inertinite has a high carbon and a low oxygen and hydrogen content (van Krevelen 1993). The average reflectance and structure of semifusinite, a maceral of the inertinite group, are similar to that of humotelinite/vitrinite and fusinite (ICCP 2001). The higher the aromatic factor, the smaller the weight loss of the sample during heating. The chemical composition of ash has a limited impact on the syngas composition. The mentioned impact is observed only for SiO₂, CaO, TiO₂, and Cr₂O₃. The degree of the conversion decreases with increasing SiO₂ content in lignite sample. On the other hand, higher CaO content is related to higher weight loss of lignite during heating. This is associated with the thermal conversion of minerals forming the ash. Carbonate minerals, such as calcite, break down at temperature of 950 °C.

In addition, it has been shown that the hydrogen and CO contents in the gas in a temperature range of 600–950 °C and the CO content in the gas in a temperature range of 950–1050 °C increase with increasing weight losses during heating. An inverse relationship is observed in the case of CO₂, H₂S, and gas density; their content in the syngas decreases with increasing weight losses during heating.

Conclusion

The main objective of this experimental study was to determine the suitability of lignite to the gasification process in CO₂ atmosphere. The study used various lithotypes of humic lignite. It has been confirmed that the composition of lignite affects the responsiveness and quality of the produced syngas.

In addition, the impact of the petrographic composition of the produced syngas has also been confirmed. When it comes to the petrographic composition, it has been found that humic coal is ideally suited for the gasification process due to its chemical structure. It has been confirmed that lignite is significantly converted already at a temperature of 600 °C. In addition, it has been shown that xylite, which is mainly made of porous textinite, is more prone to gasification. The lowest efficiency of gasification was found in the case of detritic coal, mainly made of attrinite and densinite. The most negative impact on the composition of the produced syngas is attributed to the increased amounts of macerals of the inertinite group, mainly semifusinite. These macerals increase the content of undesirable CO and CO₂. The increased ash content negatively affects the reaction speed and the quality of the produced syngas. The weight loss of the sample during heating decreases with increase in aromatic factor.

There are two phases of increased conversion in the case of coal with a higher degree of coalification and gelification; their nature is similar to those observed in medium-rank coals. The highest gas flow during the gasification of ortho-lignite is observed at temperatures in the range of 900–1050 °C, where aromatic bonds break. However, the process itself and the usefulness of the coal for the gasification process are affected mainly by moisture and ash content. They form ballast that hinders the gasification process. Therefore, when examining the suitability of the lignite for the gasification process, it is necessary to perform not only the proximate and ultimate analyses, but also the analysis of petrographic composition.

Acknowledgements The author would like to thank the employees of the CLP-B in Jastrzębie-Zdrój, Wojciech Szulik, and Karol Szymura, for carrying out the experiment. This paper was supported by the Polish National Science Centre (NCN), under research project awarded by Decision No. DEC-2013/09/D/ST10/04045 and Dean's Grant No. 15.11.140.014.

Open Access This article is distributed under the terms of the Creative Commons Attribution 4.0 International License (<http://creativecommons.org/licenses/by/4.0/>), which permits unrestricted use, distribution, and reproduction in any medium, provided you give appropriate credit to the original author(s) and the source, provide a link to the Creative Commons license, and indicate if changes were made.

References

- Akanksha, Singh AK, Mohantya D, Jena HM (2017) Characterization of lignite for underground coal gasification in India. *Energy Sour Part A Recover Utilization Environ Eff* 39:1762–1770. <https://doi.org/10.1080/15567036.2017.1352630>
- Bielowicz B (2012) A new technological classification of low-rank coal on the basis of Polish deposits. *Fuel* 96:497–510. <https://doi.org/10.1016/j.fuel.2011.12.066>
- Borrego AG, Alvarez D, Menéndez R (1997) Effects of inertinite content in coal on char structure and combustion. *Energy Fuels* 11:702–708. <https://doi.org/10.1021/ef960130m>
- Chmielniak T, Sobolewski A, Tomaszewicz G (2015) CO₂-enhanced coal gasification. Experience of the Institute for Chemical Processing of Coal Zgazowanie węgla przy wykorzystaniu CO₂ jako czynnika zgazowującego. *Doświadczenia IChPW. PRZEMYSŁ CHEMICZNY* 1:16–22. <https://doi.org/10.15199/62.2015.4.1>
- Cronauer DC, Joseph JT, Davis A et al (1992) The beneficiation of Martin Lake Texas lignite. *Fuel* 71:65–73. [https://doi.org/10.1016/0016-2361\(92\)90194-S](https://doi.org/10.1016/0016-2361(92)90194-S)
- Czarnecki L, Frankowski R, Ślusarczyk G (1992) Syntetyczny profil litostratygraficzny rejonu złoża Bełchatów dla potrzeb Bazy Danych Geologicznych. *Górnictwo Odkrywkowe* 3–4:12–22
- Diessel CF (1986) On the correlation between coal facies and depositional environments. In: *Proceedings of the 20th symposium on advances in the study of the Sydney Basin*, Department of Geology, University of Newcastle, pp 19–22
- Furimsky E, Palmer ADD, Kalkreuth WDD et al (1990) Prediction of coal reactivity during combustion and gasification by using petrographic data. *Fuel Process Technol* 25:135–151. [https://doi.org/10.1016/0378-3820\(90\)90101-W](https://doi.org/10.1016/0378-3820(90)90101-W)

- Hashimoto K, Miura K, Xu J-J et al (1986) Relation between the gasification rate of carbons supporting alkali metal salts and the amount of oxygen trapped by the metal. *Fuel* 65:489–494. [https://doi.org/10.1016/0016-2361\(86\)90038-4](https://doi.org/10.1016/0016-2361(86)90038-4)
- Higman C, van der Burgt M (2008) *Gasification*. Gulf Professional Pub./Elsevier Science
- ICCP (2001) The new inertinite classification (ICCP System 1994). *Fuel* 80:459–471. [https://doi.org/10.1016/S0016-2361\(00\)00102-2](https://doi.org/10.1016/S0016-2361(00)00102-2)
- Kalaitzidis S, Bouzinos A, Papazisimou S, Christanis K (2004) A short-term establishment of forest fen habitat during Pliocene lignite formation in the Ptolemais Basin, NW Macedonia, Greece. *Int J Coal Geol* 57:243–263
- Kasiński J, Mazurek S, Piwocki M (2006) Valorization and ranking, list of lignite deposits in Poland. *Prace Państwowego Instytutu Geologicznego* 187:79
- Kasiński J, Piwocki M, Sadowska E, Ziemińska-Tworzydło M (2010) Lignite of the Polish Lowlands Miocene: characteristics on a base of selected profiles. *Biuletyn Państwowego Instytutu Geologicznego* 439:99–154
- Kurtz R (1981) Eigenschaften der rheinischen Braunkohle und ihre Beurteilung als Roh- und Brennstoff. *Fortschr Geol Rheinl Westfal* 29:381–426
- Kwiecińska B, Wagner M (1997) Classification of qualitative features of brown coal from Polish deposits according to petrographical, chemical and technological criteria. *Wydawnictwo Centrum PPGSMiE PAN, Kraków*
- Ladner WR (1988) The products of coal pyrolysis: properties, conversion and reactivity. *Fuel Process Technol* 20:207–222. [https://doi.org/10.1016/0378-3820\(88\)90021-5](https://doi.org/10.1016/0378-3820(88)90021-5)
- Miura K, Xu J-J, Tezen Y et al (1987) Gasification reactivity of various demineralized coals. *J Fuel Soc Jpn* 66:264–272. <https://doi.org/10.3775/jie.66.264>
- Ozer M, Basha OM, Stiegel G, Morsi B (2017) Effect of coal nature on the gasification process. In: *Integrated gasification combined cycle (IGCC) technologies*. Elsevier, pp 257–304
- PGI-NRI (2017) PGI-NRI. <http://geoportal.pgi.gov.pl/surowce>
- Pickel W, Kus J, Flores D et al (2017) Classification of liptinite—ICCP system 1994. *Int J Coal Geol* 169:40–61. <https://doi.org/10.1016/j.coal.2016.11.004>
- Piwocki M, Ziemińska-Tworzydło M (1997) Neogene of the Polish Lowlands—lithostratigraphy and pollen-spore zones. *Geol Q* 41:21–40
- Porada S, Czernski G, Grzywacz P et al (2017a) Comparison of the gasification of coals and their chars with CO₂ based on the formation kinetics of gaseous products. *Thermochim Acta* 653:97–105. <https://doi.org/10.1016/J.TCA.2017.04.007>
- Porada S, Dziok T, Czernski G et al (2017b) Examinations of Polish brown and hard coals in terms of their use in the steam gasification process. *Gospodarka Surowcami Mineralnymi* 33:15–34. <https://doi.org/10.1515/gospo-2017-0007>
- Russell NJ, Barron PF (1984) Gelification of Victorian tertiary soft brown coal wood. II. Changes in chemical structure associated with variation in the degree of gelification. *Int J Coal Geol* 4:119–142. [https://doi.org/10.1016/0166-5162\(84\)90011-9](https://doi.org/10.1016/0166-5162(84)90011-9)
- Sakawa M, Sakurai Y, Hara Y (1982) Influence of coal characteristics on CO₂ gasification. *Fuel* 61:717–720. [https://doi.org/10.1016/0016-2361\(82\)90245-9](https://doi.org/10.1016/0016-2361(82)90245-9)
- Shibaoka M (1982) Behaviour of huminite macerals from Victorian brown coal in tetralin in autoclaves at temperatures of 300–380 °C. *Fuel* 61:265–270. [https://doi.org/10.1016/0016-2361\(82\)90123-5](https://doi.org/10.1016/0016-2361(82)90123-5)
- Solomon PR, Hamblen DG (1985) *Pyrolysis. Chemistry of coal conversion*. Springer, New York, pp 121–251
- Solomon PR, Fletcher TH, Pugmire RJ (1993) Progress in coal pyrolysis. *Fuel* 72:587–597. [https://doi.org/10.1016/0016-2361\(93\)90570-R](https://doi.org/10.1016/0016-2361(93)90570-R)
- Speight JG (2016) *Chemistry and technology of coal*, 3rd edn. CRC Press, Boca Raton
- Stach E, Mackowsky M-T, Teichmüller M et al (1982) *Stach's textbook of coal petrology*
- Stankiewicz BA, Krüge MA, Mastalerz M (1996) A geochemical study of macerals from a Miocene lignite and an Eocene bituminous coal, Indonesia. *Org Geochem* 24:531–545. [https://doi.org/10.1016/0146-6380\(96\)00038-1](https://doi.org/10.1016/0146-6380(96)00038-1)
- Süss M, Budde K, Müller WD (1968) Rohstoffliche Einflussfaktoren auf die Güte des BHT-Kokes aus Niederlausitzer Braunkohlen. *Freiberger Forschungsh A* 423:59–70
- Sýkorová I, Pickel W, Christanis K et al (2005) Classification of huminite—ICCP System 1994. *Int J Coal Geol* 62:85–106
- Taylor GH, Glick DC (1998) *Organic petrology: a new handbook incorporating some revised parts of Stach's textbook of coal petrology*. Gebrüder Borntraeger, Berlin
- Taylor GH, Shibaoka M, Liu S (1982) Characterization of huminite macerals. *Fuel* 61:1197–1200. [https://doi.org/10.1016/0016-2361\(82\)90019-9](https://doi.org/10.1016/0016-2361(82)90019-9)
- Teng YY, Liu YZ, Liu QS, Li CQ (2016) Macerals of Shengli lignite in inner Mongolia of China and their combustion reactivity. *J Chem* 2016:1–7. <https://doi.org/10.1155/2016/2513275>
- Tremel A, Spliethoff H (2013) Gasification kinetics during entrained flow gasification—Part II: intrinsic char reaction rate and surface area development. *Fuel* 107:653–661. <https://doi.org/10.1016/j.fuel.2012.10.053>
- van Krevelen DW (1993) *Coal—typology, physics, chemistry, constitution*. Elsevier, Amsterdam

Publisher's Note Springer Nature remains neutral with regard to jurisdictional claims in published maps and institutional affiliations.